Postprint of: Śmietana M., Koba M., Sezemsky P., Szot-Karpińska K., Burnat D., Stranak V., Niedziółka-Jönsson J., Bogdanowicz R., Simultaneous optical and electrochemical label-free biosensing with ITO-coated lossy-mode resonance sensor, Biosensors and Bioelectronics, Vol. 154 (2020), 112050, DOI: 10.1016/j.bios.2020.112050

Simultaneous optical and electrochemical label-free biosensing with ITO-coated lossy-mode resonance sensor

Mateusz Śmietana[1,*] Marcin Koba[1,2], Petr Sezemsky[3], Katarzyna Szot-Karpińska[4], Dariusz Burnat[1], Vitezslav Stranak[3], Joanna Niedziółka-Jönsson[4], and Robert Bogdanowicz[5]

[1] Warsaw University of Technology, Institute of Microelectronics and Optoelectronics, Koszykowa, 75, Warszawa, Poland

[2] National Institute of Telecommunications, Szachowa 1, 04-894 Warszawa, Poland

[3] University of South Bohemia, Institute of Physics and Biophysics, Branisovska 1760, 370 05 Ceske Budejovice, Czech Republic

[4] Polish Academy of Sciences, Institute of Physical Chemistry, Kasprzaka 44/52, 01-224 Warszawa, Poland

[5] Gdansk University of Technology, Faculty of Electronics, Telecommunications and Informatics, Narutowicza 11/12, 80-233 Gdańsk, Poland

*Corresponding author: M.Smietana@elka.pw.edu.pl +48222346364

Abstract

In this work we discuss a new label-free biosensing device based on indium tin oxide (ITO) coated section of a multimode optical fiber fused silica core. The sensor has been used to optical measurements also simultaneously interrogated electrochemically. Due to optimized thickness and optical properties of ITO film, a lossy-mode resonance (LMR) could be observed in the optical domain, where electrical properties of the film allowed for application of the sensor as a working electrode in an electrochemical setup. It has been confirmed that the LMR response depends on optical properties of the external medium, as well as potential applied to the electrode during cyclic voltammetry. After the ITO surface functionalization with amine groups and covalently attached biotin, the device has been applied for label-free biosensing of avidin in both the domains simultaneously. On the example of biotin-avidin detection system it was demonstrated that when avidin concentration increases a decrease in current and increase in LMR wavelength shift were recorded in electrochemical and optical domain, respectively. Both optical and electrochemical responses follow the protein interaction process, and thus can be used as cross-verification of the readouts. Moreover, an extended information has been

achieved comparing to solely electrochemical interrogation, i.e., the grafting process of biotin and avidin was directly monitored optically displaying individual steps of an incubation procedure.

Keywords: optical fiber sensor, lossy-mode resonance, thin film, indium tin oxide (ITO), electrochemistry, label-free biosensing, multi-domain sensing

1. Introduction

Various biosensing instrumentations and procedures have been under intensive development in the recent years [1]. Combined efforts of both scientific and industrial communities are focused on improving functional properties of biosensors, mainly such as sensitivity, specificity, detection time, and cross-sensitivity, as well as reduction of sensor fabrication costs [2]. When high sensitivity is expected, the sensing instrumentation is often quite sophisticated and exceeds requirements as these for a simple strip test [3]. When detection time is crucial, such biological procedures as florescent labeling or biomaterial amplification can be pointed out as the most time-consuming [4, 5, 6]. That is why there is a significant interest in developing label-free biosensing methods where biological target is selectively recognized by receptor usually immobilized to the sensor's surface, and changes in density/mass at the surface are detected [7].

The biosensors may be interrogated in many domains, which mainly include optical, electrical and mechanical [8]. There are advantages of each of the interrogation schemes, e.g., when optical interrogation is employed, the biosensing procedure can be often monitored in a real time, and when in turn electrochemical (EC) procedures are applied, a high sensitivity can be expected [9]. Optical biosensors show limited capability to identify a single target without separation of possible interfering agents. In turn, the EC interrogation allows for reaching deep insight into biochemical reactivity of analytes. EC additionally offers a wide range of spatially localized electrografting reactions enabling site-selective control of the surface chemistry (e.g. antibody grafting, click-chemistry) for selective recognition of biocompounds. Combining both optical and EC studies make possible to deliver additional quantitative information and unique insight into biochemical activity, what is unreachable with optical detection alone.

For only a few sensors the interrogation in more than one domain is possible at the same time [10]. The multi-domain sensing concept may allow for cross-verification of the readouts and reduce a number of false-positive results, enhance detection range or deliver more information about the analyzed biological target than when interrogated in a single domain. An example of successful multi-domain sensing includes readouts coming from surface plasmon resonance (SPR) effect together with EC response (EC-SPR). For this purposes gold-coated glass slides [11, 12] or fused silica-based optical fiber structures [13] are typically used as sensors. While SPR empowers monitoring of changes of optical

properties in proximity of the gold surface, the same gold film is used as an electrode, and thus it can be electrochemically modified or interrogated. The advantages of using optical fiber sensor over a glass slide include compact sensor size, flexibility in the electrode positioning in the tested solution, as well as immunity to electromagnetic interference, which in many cases may disturb the readout. Optical fiber sensors usually offer low limit of detection along with capability to investigate low volumes of analytes and a needle-like shape of the sensor.

Other multi-domain sensing concepts employs also EC-active, but optically transparent thin films. The requirements for such applications can be fulfilled, e.g., by some doped tin oxides, such as indium tin oxide (ITO) [14] or conductive carbon-based films, such as boron-doped diamond [15]. Due to the transparency, the electrode can also be interrogated optically in a broad spectral range. This makes it possible to gain more information about the investigated solution in comparison to single-domain analysis [16]. In this case, EC is the most often applied method for sensor surface functionalization or modification, e.g., by electropolymerization [17, 18]. Both the combined sensing concepts, namely EC-SPR and spectroelectrochemistry are widely explored. Some other reported multi-domain label-free biosensing architectures combine EC with optical ring resonators [19], optical waveguides [20], localized SPR [21], as well as micro-cantilever resonators with Raman spectroscopy [22].

In this work we discuss the use of ITO-coated optical fibers for label-free opto-EC biosensing. Optical properties and thickness of ITO film deposited on a short section of a multimode fused silica optical fiber core made appearing a lossy-mode resonance (LMR) possible [23]. The properties of the resonance observed in the fiber transmission spectrum depends on optical properties, that include refractive index (RI) of medium surrounding the ITO film. The resonant effect obtained here for sensing purposes thanks to the ITO overlay, allows for focusing on resonance wavelength as a parameter, what mitigates error coming from optical power fluctuations. This differs our sensing concepts from many other concepts reported up to date employing ITO-coated optical fiber, where due to lack of resonance effect just absorption has been measured [16, 17, 18, 24, 25]. When electrical potential is applied to the ITO film in EC setup, the properties of the resonance are influenced by composition of the electrolyte surrounding the sensor [26, 27]. For the ITO-LMR sensor, the impact of EC-polymerized ketoprofen [28] or PDOT:PSS [29] on the transmitted optical spectrum has been already reported. In this work we discuss for the first time the results of dual-domain (optical and EC) label-free biosensing experiment based on ITO-LMR sensor. Comparing to other fiber-based sensor interrogated in multiple domains, such as fiber-grating-based devices [13, 30, 31], the approach stands out with simple and possible for mass production fabrication process.

2. Experimental details

2.1 Fabrication of the sensor

The sensor fabrication procedure has been described in details in [32]. Shortly, a 2.5 cm-long section of polymer-clad silica optical fiber core (400 µm core diameter) has been coated with ITO using RF magnetron sputtering. We used 3" ITO target (In_2O_3-SnO_2 - 90/10 wt% and purity of 99.99%) sputtered at 150 W in Ar atmosphere at pressure of 0.5 Pa. The fibers were located 20 cm away from the target surface and rotated during the deposition to maintain uniformity of the film around the fiber. Before further processing and measurements of the ITO-LMR sensors, the fiber end-faces were cleaved for efficient coupling with input and output fibers. The ITO thickness reached 350 nm and it made appearance of the second order LMR in the investigated spectral range possible [32].

2.2 Optical and electrochemical measurements

The optical transmission (T) has been investigated using USB4000 spectrometer and HL-2000 tungsten light source, both from Ocean Optics. The optical data acquisition and processing has been controlled using custom Matlab script allowing to save full available optical spectrum (λ=350-1050 nm) approx. every 1.5 s. The integration time was set to 100 ms. Optical response of the ITO-LMR sensor to external RI has been investigated using water/glycerin solutions with RI varying from n_D=1.3330 to 1.45 RIU. The RI of the solutions was each time verified using Reichert AR200 automatic refractometer.

Combined optical and EC responses were acquired using a custom measurement cell able to accommodate the ITO-LMR sensor that was electrically connected via copper tape away from the core section and sealed using two silicone gaskets [32]. The EC measurements were performed in controlled environment (temperature: 22 degC, humidity 45%) using PalmSens Emstat3+ potentiostat supported by a PSTrace 5.4 software and connected to three electrodes, namely the ITO-LMR sensor, an Ag/AgCl 0.1M NaCl and a platinum wire. They were submerged in the measurement cell and used as a working (WE), reference (RE) and counter electrode (CE), respectively. During the experiment the electrodes were monitored for any contact between them. The cyclic voltammograms (CV) were recorded at 20 mV/s scan rate in the potential (*E*) ranging from -1 to 1.5 V. Both, scan rate and the range of *E* were chosen as a result of our preliminary tests and found as the most suitable for simultaneous EC and optical detection. We are aware that the response from the redox probe used in this experiment can be also observed in a way narrower *E* range. However, the wide *E* window (from -1 V to 1.5 V) was intentionally applied to get more information from the experiment, such as how the changes in the *E* influence the optical response. It must also be mentioned, that ITO electrodes are EC stable within the applied potential range. All the measurements were carried in phosphate buffered saline (PBS, pH 7.4) as well as PBS containing 1 mM 1,1-ferrocenedimethanol ($Fc(CH_2OH)_2$) as a redox probe. PBS tablets

were bought from BioShop®Canada Inc., and contained 137 mM NaCl, 2.7 mM KCl, and 10 mM phosphate buffer, pH 7.4. Schematic representation of the applied measurement setup is shown in Fig. 1.

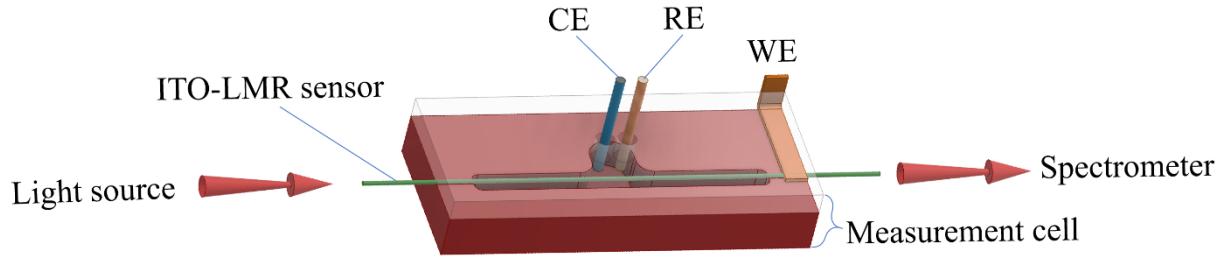

Fig. 1. Schematic representation of combined optical and electrochemical (EC) measurements performed with ITO-LMR sensor installed in a custom-made measurement cell. Instalments of reference (RE), counter (CE) and ITO-LMR sensor as a working electrode (WE) were marked. The sensor was connected to the potentiostat via copper tape and submerged in the electrolyte as well as the other electrodes.

2.3 ITO surface functionalization and biosensing procedure

For the biosensing experiment we followed the procedure as the one for protein sensing described in details in [33]. Shortly, a 30 µL of a silane precursor (3-aminopropyltriethoxysilane, APTES) and a 10 µL of catalyst (triethylamine) were used for functionalization. The fiber samples were exposed to the precursor and the catalyst vapors in a desiccator at room temperature for 2 h under argon atmosphere, and later cured for 48 h to form the amine layer (ITO-NH_2).

Next, a receptor - biotin (1 mg/mL in PBS) was chemically bonded to ITO-NH_2, like in [Biosensors and Bioelectronics 93 (2017) 102–109]. The carboxylic group of biotin was activated in N-(3-dimethylaminopropyl)- N'-ethylcarbodiimide hydrochloride (EDC, 4 mg/mL in PBS) for 15 min. Later, the fiber samples with ITO-NH_2 on their surfaces were immersed in the solution of activated biotin and left for 30 min at room temperature, then thoroughly washed with PBS. This was followed by addition of target protein – avidin with different concentrations, i.e., 0.1 µg/mL, 1 µg/mL, 10 µg/mL, and 100 µg/mL, all in PBS. The biotin-terminated samples were immersed in solutions from the lowest to the highest avidin concentration, left for 30 min, then extensively washed with PBS, and finally measured in PBS.

3. Results

3.1. ITO-LMR sensor parametrization

The ITO-LMR sensors revealed to be sensitive to external RI (n_{ext}) [23, 34]. As a result of increase in n_{ext} the resonance shifts towards longer wavelengths (Fig. 2(a)). A set of parameters can be investigated in the spectrum and used for quantitatively determining the RI sensitivity, i.e., shift of the resonance wavelength (λ_R) or T changes at a selected wavelength (Fig. 2(b)). In this work T at λ=630 nm (T_{630}) has

been chosen. Both parameters, namely λ_R and T_{630} changes significantly with n_{ext}. For the investigated case when the $d\lambda_R/dn_{ext}$ is considered, it increases from about 320 nm/RIU to 800 nm/RIU at 1.34 and 1.43 RIU, respectively. According to results of LMR-based biosensing experiment [35], such sensitivity makes it possible to monitor bio-overlay growth on the sensor's surface. When the precision in determination of λ_R is limited, as it is for simple spectrometers, the dT_{630}/dn_{ext} can be alternatively used. It offers higher resolution in identification of changes taking place at the ITO surface. One must be aware that when solely power-based interrogation is applied the result may be highly influenced by e.g. light source power fluctuations. That is why in this work where possible both parameters are discussed together. It facilitates identification of sources of errors more feasible than in case of single power interrogation. Moreover, as it will be shown in section 3.4, the identification of surface changes can be enhanced when additionally electrochemical modulation is implemented.

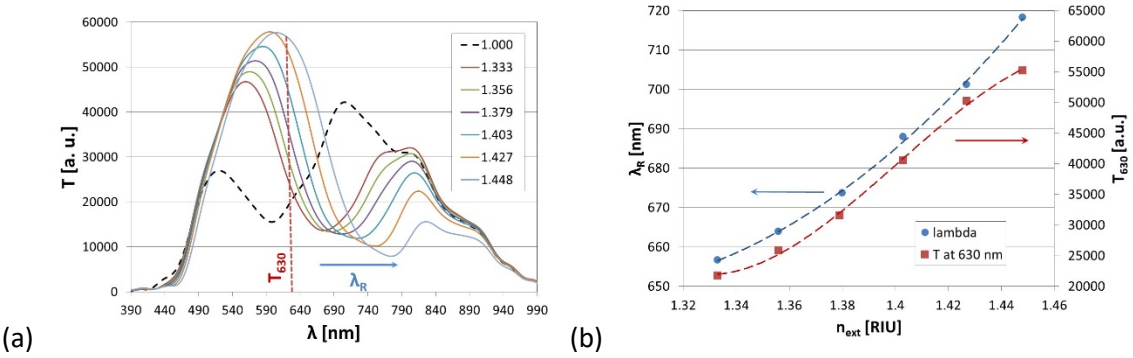

Fig. 2. Response of the ITO-LMR sensor to change in n_{ext} between 1 and 1.45 RIU, where (a) shows transmission spectrum and (b) corresponding shift in resonance wavelength and transmission at λ=630 nm for measurements in various aqueous solutions.

Next, *E* has been applied to the ITO-LMR sensor when it was immersed in PBS. As shown in Fig. 3, the increase and the decrease in *E* induces changes of both λ_R and T_{630}. The changes in the optical response while sweeping the potential are caused by variation in external RI of both the ITO overlay and the electrolyte in the closest vicinity of the ITO-LMR electrode. The applied potential alternates the number of free carriers in the ITO overlay, which, in agreement with the Drude-Lorentz model [G.T. Reed, C.E. Jason Png, Silicon optical modulators, Mater. Today. 8 (2005) 40–50. doi:10.1016/S1369-7021(04)00678-9], directly affects its real part of RI (n) as well as the imaginary part of RI (*k*) [A1]. Also, the double-layer formed on ITO, after immersion into the electrolyte, will be rearranged by repelling and attracting counterions with the sweeping potential [S. Grimnes, Ø.G. Martinsen, S. Grimnes, Ø.G. Martinsen, Electrodes, in: Bioimpedance Bioelectr. Basics, Elsevier, 2015: pp. 179–254. doi:10.1016/B978-0-12-411470-8.00007-6.], which directly influences the external RI in the closest vicinity of ITO surface. Such behavior for multi-domain measurements of ITO-coated long-period fiber grating (LPFG) was previously

observed by us [31]. For the ITO-LMR sensor, contrary to LPFG device, the changes are well visible at both the negative and the positive potentials. A hysteresis for both the selected parameters can be observed. In the applied *E* range, the λ_R alters by over 60 nm, what is comparable to the shift recorded during change in n_{ext} from 1.33 to 1.45 RIU. It can be clearly seen here that due to limited resolution of the used spectrometer in wavelength domain and high sensitivity in determining changes in *T*, tracing of T_{630} may offer more accurate readouts (smoother curves) than when shift in λ_R is analyzed.

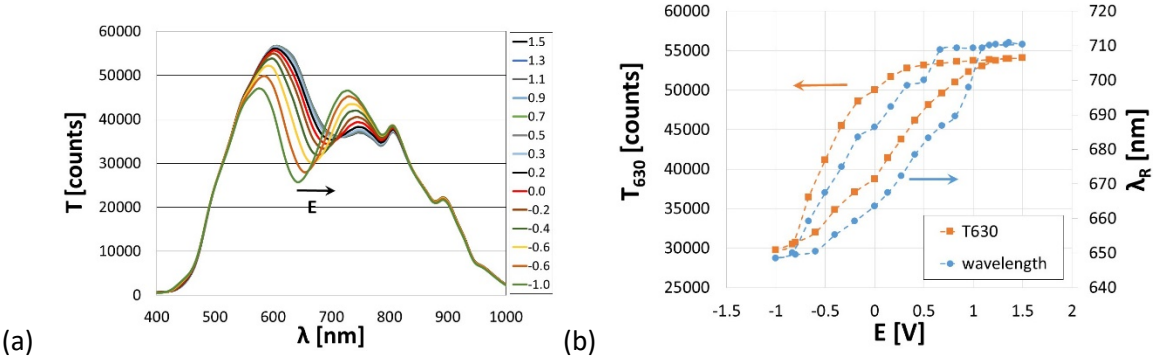

Fig. 3. Response of the ITO-LMR sensor to applied potential (*E*) varying between 0 V → 1.5 V → -1 V → 0 V, where (a) shows transmission (*T*) spectrum and (b) corresponding shift in resonance wavelength and transmission at λ=630 nm. PBS was used as an electrolyte and the scan rate was set to 20 mV/s.

3.2. Monitoring of biological binding events

Meaningful electrochemical analysis done according to label-free biosensing concept is limited to the steps of the procedure, which follow those aiming to remove physically adsorbed biological material. When the results for these steps are compared, the only parameter influencing the measurement should be related to binding events on the sensor surface. At these steps PBS or more often other buffer solution containing redox probes are used as an electrolyte, which allow for comparing between the steps the current resulting from oxidation or reduction reactions taking place at surface of the electrode. The advantage of introducing optical domain in this measurements is capability for in-situ monitoring of the sensor surface during every step of the biosensing procedure, which also include incubation process.

In Fig. 4, results of incubation monitoring at selected steps of the procedure are shown. For clearer presentation of the results the T_{630} has been normalized. In Fig. 4(a) and 4(c) initial (start) and final (stop) spectra recorded for two incubation steps (1 µg/mL and 100 µg/mL concentration of avidin, respectively) were shown. Both the considered parameters, namely λ_R and $T_{630}/\max(T_{630})$ shift toward higher values with incubation time (Fig. 4(b) and 4(d)), what correspond to the increase in n_{ext}, or in other words densification of the medium in proximity of the sensor's surface. As well as in the case of above investigated influences of *E* and n_{ext}, changes in T_{630} can be better identified here. For incubation in the highest avidin concentration (100 µg/mL), the λ_R and $T_{630}/max(T_{630})$ increase by about 0.5 nm and

2%, respectively (Fig. 4(d)). It can be clearly seen that in case of 100 µg/mL avidin, the increase in λ_R and $T_{630}/max(T_{630})$ saturates after approx. 130 measurements, what corresponds to incubation time of 20 minutes. After extensive washing of the sensor in PBS the parameters, i.e., the λ_R and $T_{630}/max(T_{630})$, were found to increase by about 1.4 nm and 1.7%. Drop in transmission indicate that an excess of avidin, which was only physically adsorbed to the surface, has been successively removed. Observation of only λ_R shift in may be misleading due to limited resolution in wavelength of the used spectrometer.

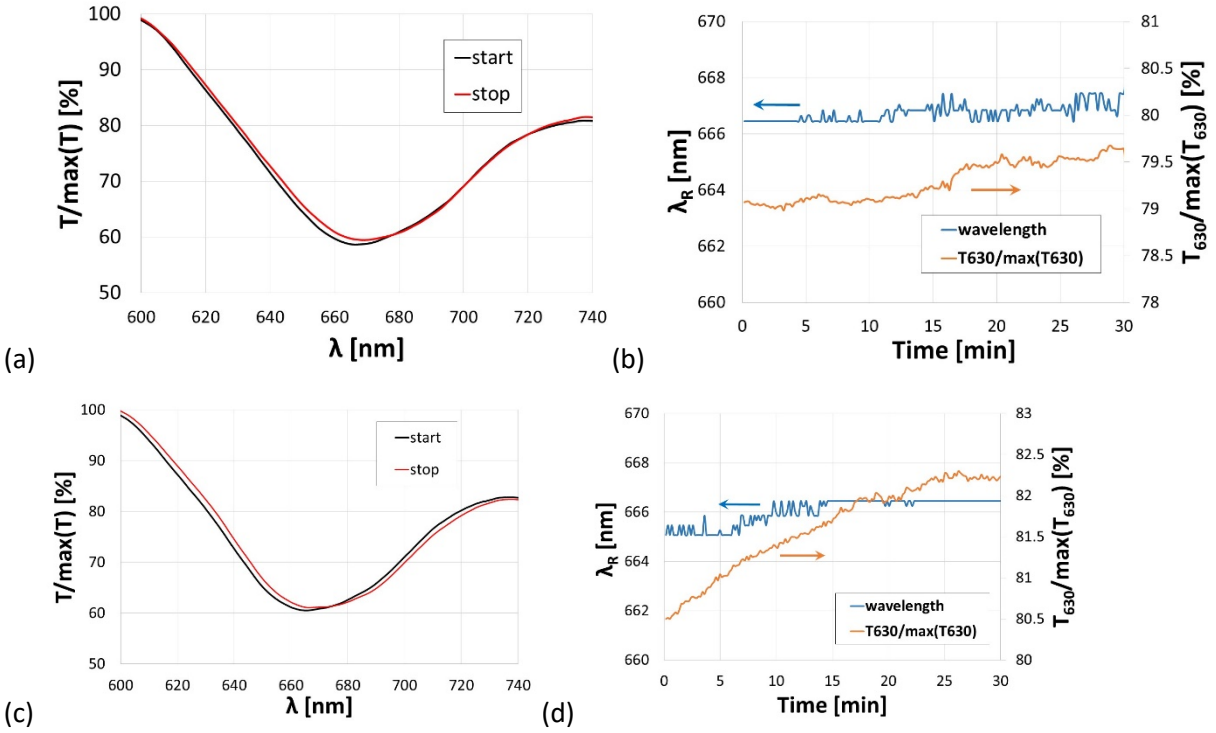

Fig. 4. Normalized initial (start) and final (stop) spectra acquired for 30 min-long incubation in 1 µg/mL (a) and 100 µg/mL (c) avidin solution. Evolution of the selected spectral parameters during the incubation is shown in (b) and (d) for 1 µg/mL and 100 µg/mL, respectively.

3.3. Detection in electrochemical domain

Fig. 5(a) depicts CV curves recorded in PBS and in presence of the redox probe ($Fc(CH_2OH)_2$) after incubation in 1 µg/mL and 10 µg/mL of avidin followed by extensive washing in PBS. In presence of $Fc(CH_2OH)_2$, two current peaks were recorded at *E* of about 0 V and 0.7 V, that correspond to reduction and oxidation processes, respectively. As a result of incubation in the solutions containing biological compounds, a drop of current at $E > 0.5$ *V* was observed. The drop was detected for both PBS and $Fc(CH_2OH)_2$. The CV curves recorded in PBS after sensor washing for all the steps of the experiment have been shown in Fig. 5(b). The decrease in current corresponds to elevated resistance of the interface, i.e., charge transfer blocking by the biomolecules immobilized at the functionalized ITO surface [37].

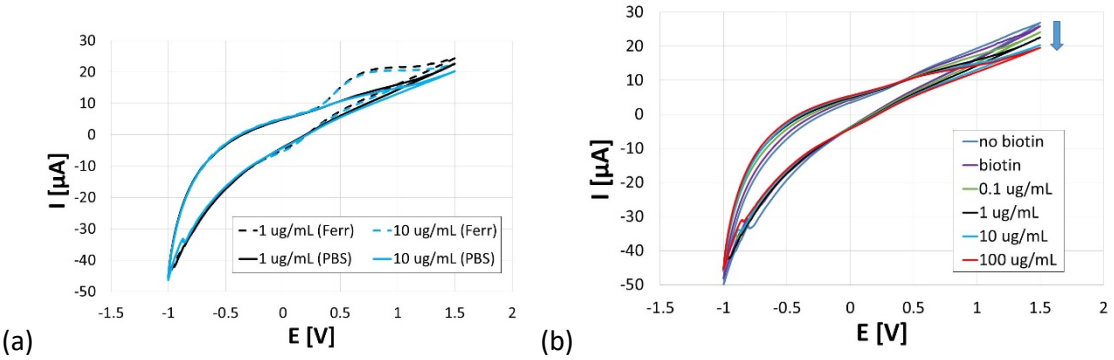

Fig. 5. CV curves recorded after incubation in solutions containing biological compounds and washing in PBS, where (a) shows results obtained in PBS and 1 mM $Fc(CH_2OH)_2$/PBS (Ferr) for two selected avidin concentrations and (b) shows results in PBS for all steps of the experiment. Arrow in at E=1.5 V in (b) shows the drop in current. Scan rate was set to 20 mV/s.

ITO has been widely applied as an electrode material, especially when together with electrochemical also spectrometric measurements are performed [14]. In those measurements typically ITO-coated glass slides are used, where ITO is thermally annealed as a part of post-deposition procedure to improve electrical properties of the films [36]. In case of ITO-coated fibers with polymer cladding the high-temperature annealing is hardly possible due to low temperature resistance of the polymer. That is why the investigated ITO films may show slightly lower electrochemical activity analyzed in presence of $Fc(CH_2OH)_2$ than for commercially available ITO-coated glass slides [32].

3.4. Detection in optical domain

Simultaneously to interrogation in electrochemical domain, the ITO-LMR sensor was interrogated optically. In contrast to CV measurements, the optical spectrum has been acquired approx. every 1.5 s. In Fig. 6(a) the evolution in time of λ_R, as well as corresponding E is show for each step of the experiment. The E-scan (from 1.5 V to -1 V and back to 1.5 V) took approx. 250 s and for comparison purposes evolution of the λ_R was shown in line for each step of the experiment. Similarly to results shown in Fig. 3, the λ_R changes significantly with E, but here additionally the shift depends on the step of the experiment, which in turn correspond to change in the bio-overlay properties. In general, the λ_R follows the E and its total shift, observed mainly when negative potentials are applied (E < 0.5 V), increases from approx. 75 nm to 90 nm for initial measurement with no biotin attached and final step after incubation in 100 µg/mL avidin solution, respectively. Moreover, when more biological film is grafted to the surface, the λ_R better follows the decrease in E. The mentioned above differences are attributed to changes in optical properties of electrolyte at the bio-layer – ITO interface, as well as at the electrolyte – bio-overlay interface. Increase in thickness and density of the bio-overlay, where later corresponds to its RI, from electrical point of view can be interpreted as appearance of an insulating layer. When negative E is applied, the concentration of free charge carriers (electrons) in ITO increases,

what is followed by decrease in *n* and increase in *k* of the film [A6]. These changes in optical properties of ITO make the LMR shift towards shorter wavelength and increase in its depth [23]. When an insulating bio-overlay appears on the ITO surface, it increases resistance of the interface, but also induces accumulation of electrons in ITO at its interface with the bio-overlay. The accumulation additionally modifies the optical properties of ITO and enhances shift of λ_R at negative *E*. The difference between the $d\lambda_R/dE$ for decrease in *E* with growth of the bio-overlay may in turn correspond to reduced double-layer i.e., lower capacitance at the electrolyte – bio-overlay interface when biological film reduces/suppress interactions between ions in the electrolyte and the ITO surface. For quantitative determination of the sensor performance in optical domain, the λ_R at E= -1 V has been compared for different steps of the experiment (Fig. 6(b)). At low *E* values, the λ_R changes more and can be better identified than for higher *E* values, where the resonance becomes shallow (Fig. 3(a)). It can be clearly seen that for the entire experiment, i.e. from the reference step before incubation in biotin up to the one for 100 µg/mL concentration of avidin, the λ_R at E= -1 V decreases by over 17 nm, and its decrease is higher for the avidin concentration up to 1 µg/mL than for its higher concentrations. It must be noted that the shift is significantly greater than those measured during biosensing experiment based on LMR effect with no *E*-scanning applied (not shown here), where for the entire experiment the shift reached about 4 nm. When change in current at *E*= 1.5 V is compared to change in λ_R, the trends of readouts in optical and electrochemical domains correspond to each other (Fig. 6(b)). The total current decreases in the whole biosensing experiment by 8 µA.

It must be noted that in this work we investigated response of the sensor to relatively high concentrations of analytes. Our aim was to more to show a novel sensing concept and its performance in broad range of analyte concentrations than to focus on the sensor optimization towards reaching low limit of detection (LOD). It can be assumed that for the shown case the LOD corresponds with the lowest measured avidin concentration (0.1 µg/mL). However, it can be lowered when higher resolution in investigated sensing parameters is investigated in narrow range of negative potentials.

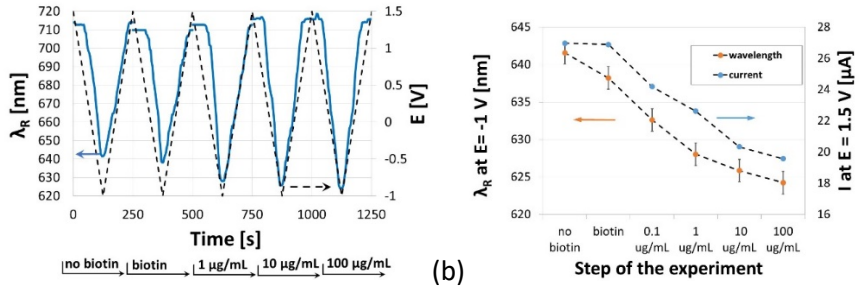

Fig. 6. (a) Influence of the *E* change on λ_R at different steps of the experiment performed in PBS. E-scan at each the experimental step took approx. 250 s and was set in line with other steps as indicated at the bottom of the plot. Optical (λ_R at *E* = -1 V) and electrochemical (*I* at *E* = 1.5 V) readouts for each step of the experiment were compared in (b).

5. Conclusion

In this paper we discuss for the first time the combined optical and electrochemical label-free biosensing based on resonant effect achieved for indium tin oxide thin film deposited on side surface of a multimode optical fiber core. In the optical domain, the measurements were based on the lossy-mode resonance effect. The electrical conductivity of the ITO overlay, in turn, made simultaneous use of the sensor as an electrode along with electrochemical investigation of its readout possible. In this work, the standard biotin-avidin biological complex was applied to verify functional properties of the sensor. While the sensor can be interrogated electrochemically only at certain steps of the experiment, which exclude incubation in liquids containing biological compounds, the LMR-based optical interrogation is possible in real-time during the entire biosensing procedure. When selected parameters of optical and electrochemical readouts are traced, the results of changes at the sensor's surface in both the domains correspond well to each other. Thus, we believe the second domain can be used to verify the results received in the first one. What is more, it has been found that the applied potential significantly enhances the optical readouts. The enhancement was achieved mainly at negative potentials applied to the electrode and corresponds to semiconducting character of the ITO film.

Small size of the ITO-LMR device, probe-like shape, which is common for electrochemical analysis, and capability for batch fabrication of the devices, can be pointed out as advantages of the proposed approach. Comparing to other opto-electrochemical sensing concepts, where metal film is used as an electrode, due to high transparency of ITO, also other spectroelectrochemical measurements can be additionally combined with the system and allow for even more in-depth analysis of a wider selection of biocompounds.

Acknowledgment

This work was supported in Poland by the National Science Centre (NCN) under grant No. 2014/14/E/ST7/00104, the National Centre for Research and Development (NCBiR) under grant No. 347324/12/NCBR/2017 and the National Agency for Academic Exchange (NAWA) under grant No. PPN/BIL/2018/1/00126, respectively. Support in optical measurements provided by Mr. Piotr Pardo is acknowledged.

References

[1] "Chemical Sensors and Biosensors: Fundamentals and Applications," Florinel-Gabriel Banica, Wiley, 1 edition, 2012.

[2] N. Wongkaew, M. Simsek, C. Griesche, and A.J. Baeumner, "Functional Nanomaterials and Nanostructures Enhancing Electrochemical Biosensors and Lab-on-a-Chip Performances: Recent Progress, Applications, and Future Perspective," Chem. Rev. vol. 119, no. 1, pp. 120-194, 2019.

[3] Z. Khoshbin, M.R. Housaindokht, A. Verdian, and M.R. Bozorgmehr, “Simultaneous detection and determination of mercury (II) and lead (II) ions through the achievement of novel functional nucleic acid-based biosensors,” Biosensors and Bioelectronics vol. 116, pp. 130-147, 2018.

[4] J. Truong, Y.-F. Hsieh, L. Truong, G. Jia, and M.C. Hammond, “Designing fluorescent biosensors using circular permutations of riboswitches,” Methods vol. 143, pp. 102-109, 2018.

[5] J.A. Kaczmarski, J.A. Mitchell, M.A. Spence, V. Vongsouthi, and C.J. Jackson, “Structural and evolutionary approaches to the design and optimization of fluorescence-based small molecule biosensors,” Current Opinion in Structural Biology vol. 57, pp. 31-38, 2019.

[6] P. Zhurauski, S.K. Arya, P. Jolly, C. Tiede, D.C. Tomlinson, P.K. Ferrigno, and P. Estrela, “Sensitive and selective Affimer-functionalised interdigitated electrode-based capacitive biosensor for Her4 protein tumour biomarker detection,” Biosensors and Bioelectronics vol. 108, pp. 1-8, 2018.

[7] M. Citartan, S.C. Gopinath, J. Tominaga, and T.H. Tang, “Label-free methods of reporting biomolecular interactions by optical biosensors”, Analyst vol. 138, no. 13, pp. 3576-3592, 2013.

[8] “Dual-Mode Electro-photonic Silicon Biosensors,” J. Juan-Colás, Springer Theses, Springer, 2017.

[9] C.M. Hill, D.A. Clayton and S. Pan, “Combined optical and electrochemical methods for studying electrochemistry at the single molecule and single particle level: recent progress and perspectives,” Phys. Chem. Chem. Phys. Vol. 15, pp. 20797-20807, 2013.

[10] J. Juan-Colás, S. Johnson, and T.F. Krauss, “Dual-Mode Electro-Optical Techniques for Biosensing Applications: A Review,” Sensors vol. 17, no. 9, pp. 2047, 2017.

[11] C. Wu, F. ur Rehman, J. Li, J. Ye, Y. Zhang, M. Su, H. Jiang, and X. Wang, “Real-Time Evaluation of Live Cancer Cells by an in Situ Surface Plasmon Resonance and Electrochemical Study”, ACS Appl. Mater. Interfaces, vol. 7, no. 44, 24848-24854, 2015.

[12] N.-F. Chiu, C.-D. Yang, C.-C. Chen, and C.-T. Kuo, “Stepwise control of reduction of graphene oxide and quantitative real-time evaluation of residual oxygen content using EC-SPR for a label-free electrochemical immunosensor”, Sensor Actuat. B-Chem. vol. 258, pp. 981-990, 2018.

[13] C. Caucheteur, T. Guo, and J. Albert, “Review of Plasmonic Fiber Optic Biochemical Sensors: Improving the Limit of Detection,” Anal. Bioanal. Chem. vol. 407, no. 14, 3883–3897, 2015.

[14] S.D. Branch, A.M. Lines, J. Lynch, J.M. Bello, W.R. Heineman, and S.A. Bryan, “Optically Transparent Thin-Film Electrode Chip for Spectroelectrochemical Sensing,” Anal. Chem. vol. 89, no. 14, pp. 7324–7332, 2017.

[15] J. Stotter, Y. Show, S. Wang, and G. Swain, “Comparison of the Electrical, Optical, and Electrochemical Properties of Diamond and Indium Tin Oxide Thin-Film Electrodes,” Chem. Mater. vol. 17, no. 19, 4880–4888, 2005.

[16] T. Okazaki, E. Shiokawa, T. Orii, T. Yamamoto, N. Hata, A. Taguchi, K. Sugawara, and H. Kuramitz, “Simultaneous Multiselective Spectroelectrochemical Fiber-Optic Sensor: Sensing with an Optically Transparent Electrode,” Anal. Chem. vol. 90, no. 4, 2440–2445, 2018.

[17] E. Eltzov, S. Cosnier, and R.S. Marks, “Biosensors Based on Combined Optical and Electrochemical Transduction for Molecular Diagnostics,” Expert Review of Molecular Diagnostics vol. 11, no. 5, pp. 533–546, 2011.

[18] T. Konry, A. Novoa, S. Cosnier, and R.S. Marks, “Development of an “Electroptode” Immunosensor: Indium Tin Oxide-Coated Optical Fiber Tips Conjugated with an Electropolymerized Thin Film with Conjugated Cholera Toxin B Subunit,” Anal. Chem. vol. 75, no. 11, pp. 2633–2639, 2003.

[19] J. Juan-Colás, A. Parkin, K.E. Dunn, M.G. Scullion, T.F. Krauss and S.D. Johnson, “The electrophotonic silicon biosensor,” Nat. Commun. vol. 7, 12769, 2016.

[20] J.H. Ghithan, M. Moreno, G. Sombrio, R. Chauhan, M.G. O'Toole, and S.B. Mendes, "Influenza virus immunosensor with an electro-active optical waveguide under potential modulation," Optics letters vol. 42, no. 7, pp. 1205-1208, 2017.

[21] T. Sannomiya, H. Dermutz, C. Hafner, J. Vörös, and A.B. Dahlin, "Electrochemistry on a Localized Surface Plasmon Resonance Sensor, " Langmuir vol. 26, no. 10, 7619-7626, 2010.

[22] J. Park, D. Bang, K. Jang, E. Kim, S. Haam and S. Na, "Multimodal label-free detection and discrimination for small molecules using a nanoporous resonator," Nature Comm. Vol. 5, 3456, 2014.

[23] I. Del Villar, M. Hernaez, C.R. Zamarreño, P. Sánchez, C. Fernández-Valdivielso, F.J. Arregui, and I.R. Matias, "Design Rules for Lossy Mode Resonance Based Sensors," Appl. Opt., vol. 51, no. 19, pp. 4298–4307, 2012.

[24] K. Imai, T. Okazaki, N. Hata, S. Taguchi, K. Sugawara, H. Kuramitz, "Simultaneous Multiselective Spectroelectrochemical Fiber-Optic Sensor: Demonstration of the Concept Using Methylene Blue and Ferrocyanide," Anal. Chem. vol. 87, no. 4, pp. 2375–2382, 2015.

[25] B.M. Beam, N.R. Armstrong, B.S. Mendes, "An Electroactive Fiber Optic Chip for Spectroelectrochemical Characterization of Ultra-Thin Redox-Active Films," Analyst vol. 134, no. 3, pp. 454–459, 2009.

[26] M. Śmietana, P. Niedziałkowski, W. Białobrzeska, D. Burnat, P. Sezemsky, M. Koba, V. Stranak, K. Siuzdak, T. Ossowski, and R. Bogdanowicz, "Study on Combined Optical and Electrochemical Analysis Using Indium-Tin-Oxide-Coated Optical Fiber Sensor," Electroanalysis vol. 31, no. 2, pp. 392-404, 2018.

[27] M. Śmietana, M. Sobaszek, B. Michalak, P. Niedziałkowski, W. Białobrzeska, M. Koba, P. Sezemsky, V. Stranak, J. Karczewski, T. Ossowski, and R. Bogdanowicz, „Optical Monitoring of Electrochemical Processes With ITO-Based Lossy-Mode Resonance Optical Fiber Sensor Applied as an Electrode," J. Lightwave Technol. Vol. 36, no. 4, pp. 954–960, 2018.

[28] R. Bogdanowicz, P. Niedziałkowski, M. Sobaszek, D. Burnat, W. Białobrzeska, Z. Cebula, P. Sezemsky, M. Koba, V. Stranak, T. Ossowski, and M. Śmietana, „Optical Detection of Ketoprofen by Its Electropolymerization on an Indium Tin Oxide-Coated Optical Fiber Probe," Sensors vol. 18, no. 5, 1361, 2018.

[29] M. Sobaszek, D. Burnat, P. Sezemsky, V. Stranak, R. Bogdanowicz, M. Koba, K. Siuzdak, and M. Śmietana M., "Enhancing electrochemical properties of ITO-coated lossy-mode resonance optical fiber sensor by electrodeposition of PEDOT:PSS," Opt. Mater. Express vol. 9, no. 7, pp. 3069-3078, 2019.

[30] R. Bogdanowicz, M. Sobaszek, M. Ficek, M. Gnyba, J. Ryl, K. Siuzdak, W.J. Bock, and M. Smietana, "Opto-electrochemical sensing device based on long-period grating coated with boron-doped diamond thin film", J. Opt. Soc. Korea vol. 19, no. 6, 705-710, 2015.

[31] M. Janczuk-Richter, M. Piestrzyńska, D. Burnat, P. Sezemsky, V. Stranak, W.J. Bock, R. Bogdanowicz, J. Niedziółka-Jönsson, and M. Śmietana, "Optical Investigations of Electrochemical Processes Using a Long-Period Fiber Grating Functionalized by Indium Tin Oxide," Sens. Actuat. B: Chem. vol. 279, pp. 223–229, 2019.

[32] P. Niedziałkowski, W. Białobrzeska, D. Burnat. P. Sezemsky, V. Stranak, H. Wulff, T. Ossowski, R. Bogdanowicz, M. Koba, and M. Śmietana, "Electrochemical performance of indium-tin-oxide-coated lossy-mode resonance optical fiber sensor," Sens. Actuat. B: Chem. vol. 301, 127043, 2019.

[33] M. Piestrzyńska, M. Dominik, K. Kosiel, M. Janczuk-Richter, K. Szot-Karpińska, E. Brzozowska, L. Shao, J. Niedziółka-Jönsson, W.J. Bock, and M. Śmietana, "Ultrasensitive tantalum oxide nano-coated long-period gratings for detection of various biological targets," Biosensors and Bioelectronics vol. 133, 8-15, 2019.

[34] K. Kosiel, M. Koba, M. Masiewicz, and M. Śmietana, "Tailoring Properties of Lossy-Mode Resonance Optical Fiber Sensors with Atomic Layer Deposition Technique," Optics & Laser Technology vol. 102, pp. 213–221, 2018.

[35] F. Chiavaioli, P. Zubiate, I. Del Villar, C.R. Zamarreño, A. Giannetti, S. Tombelli, C. Trono, F.J. Arregui, I.R. Matias, F. Baldini, "Femtomolar Detection by Nanocoated Fiber Label-Free Biosensors," ACS Sens. Vol. 3, no. 5, 936–943, 2018.

[36] I. Del Villar, C.R. Zamarreño, M. Hernaez, P. Sanchez, F.J. Arregui, I.R. Matias, “Generation of Surface Plasmon Resonance and Lossy Mode Resonance by Thermal Treatment of ITO Thin-Films,” Optics & Laser Technology vol. 69, pp. 1–7, 2015.

[37] C. Li, X. Chen, N. Wang, B. Zhang, “An ultrasensitive and label-free electrochemical DNA biosensor for detection of DNase I activity,” RSC Adv. Vol. 7, pp. 21666-21670, 2017.

[A1] X. Han, S.B. Mendes, Spectroelectrochemical properties of ultra-thin indium tin oxide films under electric potential modulation, Thin Solid Films. 603 (2016) 230–237. doi:10.1016/j.tsf.2016.02.018

[A3] G.T. Reed, C.E. Jason Png, Silicon optical modulators, Mater. Today. 8 (2005) 40–50. doi:10.1016/S1369-7021(04)00678-9

[x] Z. Ma, Z. Li, K. Liu, C. Ye, V.J. Sorger, „Indium-Tin-Oxide for High-performance Electro-optic Modulation” Nanophotonics 2015; 4:198–21